ELSEVIER

Chemical Engineering Science 61 (2006) 3386–3399

Chemical Engineering Science

www.elsevier.com/locate/ces

Estimator-based control of reactive distillation system: Application of an extended Kalman filtering

Moshood J. Olanrewaju, Muhammad A. Al-Arfaj*

Department of Chemical Engineering, King Fahd University of Petroleum & Minerals, Dhahran 31261, Saudi Arabia

Received 3 May 2005; received in revised form 28 October 2005; accepted 5 December 2005
Available online 3 February 2006

Abstract

This paper demonstrates that a state estimator can be successfully designed and implemented in a feedback control system of reactive distillation. The work of the state estimator is to provide the state compositions that are required to be used in the controller for necessary action. The control performance of a system that relies on the state estimator is examined and compared to a system that takes direct measurement from the process assuming the availability of a perfect online analyzer. It is found that the estimator-based system is robust against a moderate measurement errors and erroneous initial conditions. If the state estimator is designed from a highly erroneous process model, noisy measurements and approximate initial conditions, the use of estimator together with an online analyzer (for easily measured states) is recommended to achieve an effective control of a reactive distillation system.
© 2006 Elsevier Ltd. All rights reserved.

Keywords: Reactive distillation; State estimator; Process control

1. Introduction

Estimator-based control application has received considerable attention over the past several years. Basically, this is the problem of controlling a process where imperfect or limited information is available describing the states of the system that change considerably during the interval in which control is required. Al-Arfaj and Luyben (2000) suggested that the state estimator could be a suitable alternative to the expensive and often unreliable composition analyzer when there is a need to measure the internal composition of reactive distillation system for control purposes. In the same paper (Al-Arfaj and Luyben, 2000), the literature on control of reactive distillation system up to 2000 was summarized. Since then, several other papers have appeared in the literature that discussed the closed-loop reactive distillation.

Vora and Daoutidis (2001) studied the dynamics and control of a reactive distillation column for the production of ethyl acetate from acetic acid and ethyl alcohol. A single feed of almost equal amounts of both reactants was used. Utilizing the index two DAE model, the authors analyzed the system from a steady state and a dynamic point of view. Based on their results, the authors claimed that the process has two time scales caused by the liquid hydraulics. Motivated by this finding, a modified slow dynamics model was developed assuming that the volume of liquid on a tray approaches the weir volume instantaneously. A control structure that manipulates the reflux flow to control the acetate purity in the top and the condenser duty to control the column pressure was used. Nonlinear controllers were designed based on the two-time scale model. Those controllers performed well when the product purity setpoint was increased to 25%. On the other hand, the authors showed that linear controllers for the same configuration were able to handle only a 1% product purity change. However, the system was closed-loop unstable when a plant–model mismatch was introduced in designing the nonlinear controllers. The authors then showed that when the slow dynamics model was used, the system was closed-loop stable and performed well when the product purity increased up to 25% even if there is a plant–model mismatch.

* Corresponding author. Tel.: +966 3 860 1694; fax: +966 3 860 4234.
E-mail address: maarfaj@kfupm.edu.sa (M.A. Al-Arfaj).

0009-2509/$ - see front matter © 2006 Elsevier Ltd. All rights reserved.
doi:10.1016/j.ces.2005.12.009

Al-Arfaj and Luyben (2002a) further investigated the control structures for ethyl *tert*-butyl ether (ETBE) reactive distillation columns using two different process configurations: a design with two fresh reactant feed streams and a design with a single reactant feed. They presented an optimum design for the double-feed case. In their study, several control structures are investigated, and their effectiveness in the ETBE case is compared with that in their previous study. The results showed that the double-feed system requires the internal composition control to balance the feed stoichiometry, along with temperature control to maintain product purity. They extended their work to the study of methyl acetate reactive distillation control (Al-Arfaj and Luyben, 2002b).

Al-Arfaj and Luyben (2002c) had also demonstrated that ethylene glycol reactive distillation columns can be controlled effectively by a simple PI control scheme. Their proposed control structure achieves the stoichiometric balancing of the reactants and maintains the product purity within reasonable bounds. In their work, only simple conventional PI loops are used, no composition analyzer is required and the structure shows that it can handle large disturbances. Thus, they reported that the structure can be generally applicable to other systems that are similar to the ethylene glycol system in stoichiometry, kinetics, vapor–liquid equilibrium and design.

Bisowarno et al. (2003) developed and implemented model gain scheduling (MGS) on one-point control (product purity) of an ETBE reactive distillation column. Their control strategy employs a set of simple local models, which cover relevant operating conditions and cope with the nonlinear characteristics of the process. The simple models are then integrated by using a proper switching scheme. The authors emphasized the success of MGS in overcoming the problem of change in process gain directionality for a wide range of operating conditions, which cannot be handled well by using standard PI control with fixed parameters. Though MGS clearly provides an improved control performance for both setpoint tracking and disturbance rejection in the reactive distillation column, it demands preprogramming or online identification of the process gain. Larger values of noise can destabilize the system. The need for an estimator to maintain the primary controlled variable (e.g., product purity) was advocated especially because of feed composition changes.

Wang et al. (2003) made use of a steady-state analysis to design the control strategy of MTBE reactive distillation column. Although both the input and output state multiplicities occur in the column, the authors showed that a linear control is still possible provided controlled and manipulated variable pairings that exhibit no multiplicities could be found and the system is operated at constant reflux ratio. The keys of controlling the column are to maintain the quality of the bottom product, and to maintain the correct stoichiometric balance between the feeds. The temperature in the stripping section was controlled by manipulating the heat duty. The authors claimed that stoichiometric balance could be controlled either by a feed ratio or internal composition control scheme. However, when internal composition control is used the authors stated the need to consider the interaction between the quality control loop and the stoichiometric control loop.

Al-Arfaj and Luyben (2004), in their recent study, presented a plantwide flowsheet that contains reactive distillation column for the production of *tert*-amyl methyl ether (TAME). The flowsheet consists of one reactor, one reactive column, two conventional columns and two recycles. They discussed the importance of plantwide control and the role of reactive distillation. The reactive distillation column was found to be the central part of the whole flowsheet in terms of both the steady-state design and the dynamic controllability.

However, only a few papers have appeared in the literature on the application of state estimation schemes in reactive distillation control. Monroy-Loperena and Alvarez-Ramirez (2000) proposed an output-feedback control, which makes use of a reduced-order observer to estimate the modeling error, for a batch reactive distillation. In their proposed feedback control design for online implementation, it was assumed that only concentration measurement or estimation is the product purity. Gruner et al. (2003) designed and implemented a state observer in a nonlinear control of an industrial reactive distillation column. This observer design method does not rely on both the precise parameter values and the structure of the model equations. It is based on purely qualitative properties of the column profiles, which differ from one reactive distillation column to the other. Consequently, the observer will only work provided that those properties are present in both, the real plant and the model used for the observer design.

The aim of this paper is to demonstrate that a full-order state estimator can be successfully designed and implemented in a feedback control of reactive distillation. The work of the state estimator is to estimate the desired state compositions that are required for proper control of reactive distillation. The control performance of the system that relies on the state estimator is examined and compared to that of the system which takes direct measurement from the process assuming the availability of perfect online analyzer. The effect of measurement errors, plant–model mismatch and erroneous initial conditions on the estimator-based control system is investigated.

2. Reactive distillation dynamics

The process under consideration is a generic reactive distillation column schematically shown in Fig. 1. The system consists of N stages including a partial reboiler and a total condenser. The main column is further divided into three sections, which are stripping section (N_S), reactive section (N_{RX}) and rectifying section (N_R). The reversible elementary liquid-phase reaction occurring in the reactive zone is given as

$$A + B \Leftrightarrow C + D, \tag{1}$$

where the product C is the lightest and product D is the heaviest in the system. The reactants A and B are intermediate boilers with component A being a lighter reactant than component B. Thus, the fresh feed stream F_A containing reactant A is fed from

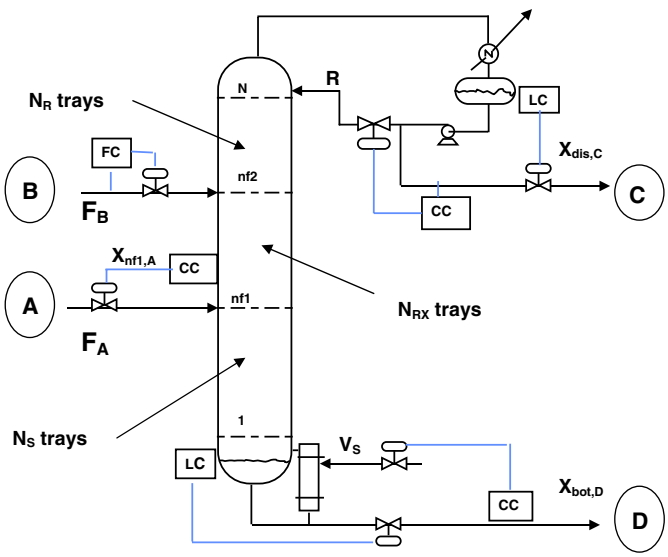

Fig. 1. Reactive distillation column.

the bottom of reactive tray, while the fresh feed F_B containing reactant B is fed at the top of the reactive zone.

2.1. The nonlinear process model

A full-order model is employed to simulate the dynamics of the reactive distillation with an ideal vapor–liquid equilibrium, reaction kinetics and physical properties. We have considered a simplified process model that presents the essential dynamics and retain the main features of a typical reactive distillation system in order to gain more insights and understanding on the generic behavior of reactive distillation without clouding the model with details pertaining to a given chemical system. The model assumptions are summarized as follows:

1. Ideal vapor–liquid equilibrium.
2. Constant liquid hold up on the trays.
3. The energy equations are neglected by assuming constant molar overflow except in the reactive zone where the vapor flowrate increases due to heat of reaction which vaporizes some liquid on each tray.
4. Constant relative volatilities. The volatilities of the components are such that

$$\alpha_D < \alpha_B < \alpha_A < \alpha_C. \tag{2}$$

5. Fixed heat of reaction and vaporization and saturated liquid feed and reflux.

The reaction rate of component j on tray is given and described by

$$R_{i,j} = \Phi_j M_i (k_{F,i} x_{i,A} x_{i,B} - k_{B,i} x_{i,C} x_{i,D}), \tag{3}$$

where Φ_j is the reaction stoichiometric factor of component j and M_i is the liquid holdup (kmol) on tray i. The dependence of reaction rate constants $k_{F,i}$ and $k_{B,i}$ on temperature T_i on reactive trays is given by the following equations:

$$k_{F,i} = a_F \mathrm{e}^{-E_F/RT_i}, \tag{4}$$

$$k_{B,i} = a_B \mathrm{e}^{-E_B/RT_i}, \tag{5}$$

where a_F and a_B are the pre-exponential factors, E_F and E_B are the activation energies. The absolute temperature T_i is evaluated using an ideal vapor–liquid equilibrium equation

$$T_i = B_{vp,1} \Bigg/ \left[A_{vp,1} - \ln \left(\alpha_1 P \Bigg/ \sum_{k=1}^{Nc} \alpha_k x_{ik} \right) \right]. \tag{6}$$

Mole balances on all of the components and the algebraic equations describing the vapor and liquid flowrates in the reactive zone give the reactive distillation model

$$\frac{\mathrm{d}x_{ij}}{\mathrm{d}t} = [L_{i+1}(x_{i+1,j} - x_{i,j}) + V_{i-1}(y_{i-1,j} - x_{i,j}) + V_i(x_{i,j} - y_{i,j}) + R_{i,j} + F_i(Z_{ij} - x_{ij})]/M_i, \tag{7}$$

$$L_i = L_{i-1} - \frac{\lambda}{\Delta H_v} \sum_{k=1}^{i-N_S-1} R_{N_S+1+k,j}, \tag{8}$$

$$V_i = V_S + \frac{\lambda}{\Delta H_v} \sum_{k=1}^{i-N_S-1} R_{N_S+1+k,j}, \tag{9}$$

where V_S is the constant vapor boilup (kmol/s) from the stripping section and V_i is the vapor flowrate (kmol/s) on tray i in the reactive zone. F_i is the feed flowrate entering the tray i. λ is the exothermic heat of reaction (cal/mol) and ΔH_v is heat of vaporizations (cal/mol). Note that the rate of reaction $R_{i,j}$ is equal to zero in all the nonreactive trays and $F_i = 0$, except at $i = \mathrm{nf1}, \mathrm{nf2}$ (feed trays). The kinetic, physical and vapor–liquid equilibrium constant parameters for this system are obtained from Luyben (2000).

The nonlinear model of reactive distillation can be represented in more compact state space vector equations of the form

$$\frac{\mathrm{d}X(t)}{\mathrm{d}t} = f(X(t), U(t), d(t); \theta), \tag{10}$$

$$Y = h(X(t); \theta), \tag{11}$$

where the $4N$-dimensional X is a vector of the state variables (liquid mole fractions in all the stages including partial reboiler and total condenser). θ represents the model constant parameters. The manipulated variables vector is represented by U while d represents the vector of disturbance variables. Y is a vector of measured output variables, which in this work are some selected column temperatures.

3. State estimator structure

The most important component of the control system studied in this work is the underlying state estimator. An extended Kalman filter (EKF), which has been the most popular estimation technique available in the literature is considered. The theory behind EKF is well established and its applications have

grown significantly in the academics and industry (Sorenson, 1985; Baratti et al., 1995, 1998; Oisiovici and Cruz, 2000). Therefore, only the brief equations as it is relevant to this work are provided. The term "extended" implies that a nonlinear model is used to develop a state estimator to observe the state variables. Based on the system model presented in Section 2, the state estimator components are formulated as

$$\frac{\mathrm{d}X(t)}{\mathrm{d}t} = f(X(t), U(t), d(t); \theta) + w(t), \tag{12}$$

$$Z = h(X(t); \theta) + v(t), \tag{13}$$

$$X(0) = X_0 + x_0\mathrm{err} \tag{14}$$

$w(t)$ is a vector of plant noise, $v(t)$ represents measurement noise vector and $x_0$err is a vector of initial conditions error. The initial conditions error is the deviation of the initial estimates from that of the real plant as obtained from the nonlinear process model. $w(t)$ and $v(t)$ are assumed to be independent white-noise sequences with the standard deviations of δ_p and δ_m, respectively. X_0 is a vector of the actual initial conditions for the system at the steady state. The initial condition estimates $X(0)$ for the state estimator models has initial conditions error ($x_0$err), which is independent of plant and measurement noise. All of these components are combined into a state estimator of the form

$$\hat{Y} = h(\hat{X}(t); \theta), \tag{15}$$

$$\hat{X}(0) = X_0 + x_0\mathrm{err}, \tag{16}$$

$$\dot{\hat{X}} = f(\hat{X}, U, d; \theta) + K[Z(X) - \hat{Y}(\hat{X})]. \tag{17}$$

The state estimator has three inputs U, d and Z and its output yields the estimated state vector $\hat{X}$. K is the gain matrix of state estimator and is evaluated using the Kalman filtering algorithm (Sorenson, 1985). In order to design a state estimator, it is a necessity that the system is observable. Considerations based on simulated studies suggest that using not less than $N/2$ temperature measurements uniformly distributed in the column is a sufficient condition to observe all of the liquid compositions in the reactive distillation under study.

The presence of both reaction and separation in reactive distillation stands as a challenge for the application of state estimation in the control of this process. In particular, more attention to obtain accurate process model (including the reaction kinetics model) and to minimize the effect of the measurement errors is to be given when state estimators are developed to be used in reactive distillation.

4. Control system configuration

Al-Arfaj and Luyben (2000) discussed many control schemes for the same system under study. In their study, it was assumed that a perfect analyzer is available to measure the composition whenever it is needed for control purposes. In this study, the control configuration of interest is the estimator-based control system, where the developed state estimator is implemented in the feedback control of reactive distillation column to estimate the inaccessible states. As shown in Fig. 2, the estimates from the state estimator will serve as input to the controller and the decision based on such feedback information is then implemented on the process. In this work, we considered the dual end control structure (see Fig. 1) in which the purities of both products are measured and controlled. In the distillate product, the composition of component C is controlled by manipulating the reflux flowrate. In the bottom, the composition of component D is controlled by manipulating the vapor boilup. The reflux-drum level is controlled by the distillate flowrate while the bottom level is controlled by manipulating the bottom flowrate.

Al-Arfaj and Luyben (2000) stated the necessity to detect an internal composition of one of the reactants in two-reactant–two-product reactive distillation column so that feedback trim can balance the feed stoichiometry. Therefore, the concentration of reactant A on the tray nf1 is measured and controlled by manipulating the fresh feed flowrate of component A. All of the composition controllers are PI except the internal composition controller which is P-only as the objective is to control the reactant A inventory. These loops are tuned by conducting relay-feedback tests to find ultimate gains and frequencies and then using the Tyreus–Luyben settings. All of the control valves are designed to be half open at the initial steady state. Therefore, all of the manipulated variables cannot increase more than twice their steady-state values.

In order to assess the performance of the estimator-based control system, two control configurations are compared as follows:

(I) *Control system CS-A*: In this control system, the desired states (liquid compositions) which will be used by the controllers are assumed to be perfectly available at any desired time using an online analyzer. This control structure is considered in the present work only to serve as a reference to which the performance of the estimator-based control system is assessed. The three composition controller equations in CS-A are of the form

$$F_A = f_A(x_{\mathrm{nf1},A}), \tag{18}$$

$$V_S = f_v(x_{\mathrm{bot},D}), \tag{19}$$

$$R = f_R(x_{\mathrm{dis},C}). \tag{20}$$

Therefore, Eqs. (10), (11) and (18)–(20) formulate the closed-loop system with perfect online analyzer for composition measurements.

(II) *Control system CS-E3*: This control system is the controller–estimator configuration and is shown in Fig. 2. The states of the process are estimated using EKF estimator and all of the three estimated controlled variables (i.e., $\hat{x}_{\mathrm{nf1},A}, \hat{x}_{\mathrm{bot},D}, \hat{x}_{\mathrm{dis},C}$) are provided to the controllers by the state estimator (see Fig. 2). Therefore, Eqs. (18)–(20) will be replaced by

$$F_A = f_A(\hat{x}_{\mathrm{nf1},A}), \tag{21}$$

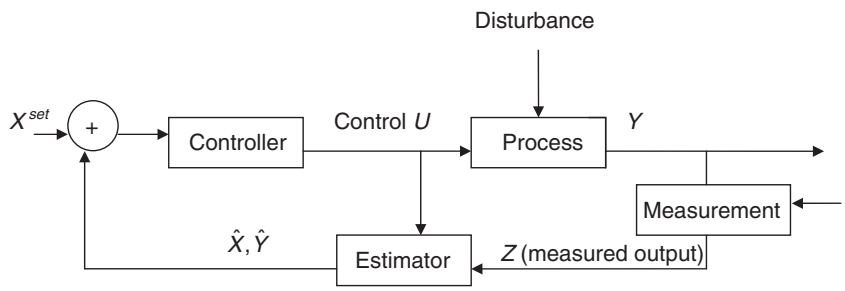

Fig. 2. The estimator-based control system configuration.

Table 1
The base steady-state conditions

	Variables	Steady-state values
Column specifications	Pressure (bar)	9
	Stripping section (N_S)	7
	Reactive section (N_{RX})	6
	Rectifying section (N_R)	7
Equilibrium data	Relative volatilities: $A/B/C/D$	4/2/8/1
Flowrates (kmol/s)	Feed rate of reactant A	0.0126
	Feed rate of reactant B	0.0126
	Vapor boil up	0.0285
	Reflux rate	0.0331
	Distillate	0.0126
	Bottoms	0.0126
X_{dis}	A	0.0467
	B	0.0033
	C	0.9500
	D	0.0000
X_{bot}	A	0.0018
	B	0.0482
	C	0.0000
	D	0.9500

$$V_S = f_v(\hat{x}_{\text{bot},D}), \tag{22}$$

$$R = f_R(\hat{x}_{\text{dis},C}), \tag{23}$$

where the $\hat{x}$ is the estimated state that comes from the state estimator described by Eqs. (15)–(17).

5. Results and discussion

A constant liquid holdup of 1 kmol in all of the trays and 10 kmol in both the partial reboiler and the total condenser are assumed throughout the simulation. Table 1 gives the summary of the steady-state operating conditions for the system under study. In this work, temperature measurements are evenly located on 11 stages out of the 22 stages. The noise-contaminated temperature measurements from the process are available (with no time delay) to the state estimator at a constant time interval. Because the process model used in the EKF algorithm is not a perfect representation of the plant, a plant noise ($\delta_p = 1\%$) and a measurement noise ($\delta_m = 10\%$) was used in the design and implementation of an extended Kalman filter, as well as in all the simulation studies.

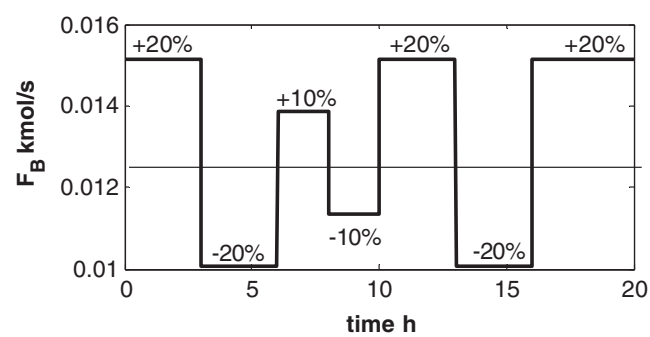

Fig. 3. A pseudo-rectangular random sequence (PRRS) forcing function on F_B.

5.1. Control performance

In order to examine the performance of the estimator-based control system, changes in feed flowrate of reactant B (F_B) and products composition setpoint are considered. The following changes of reactant B feed flowrate are made:

(1) Step changes of ±20% ($\pm\Delta F_B$).
(2) A pseudo-rectangular random sequence (PRRS) forcing function as shown in Fig. 3.

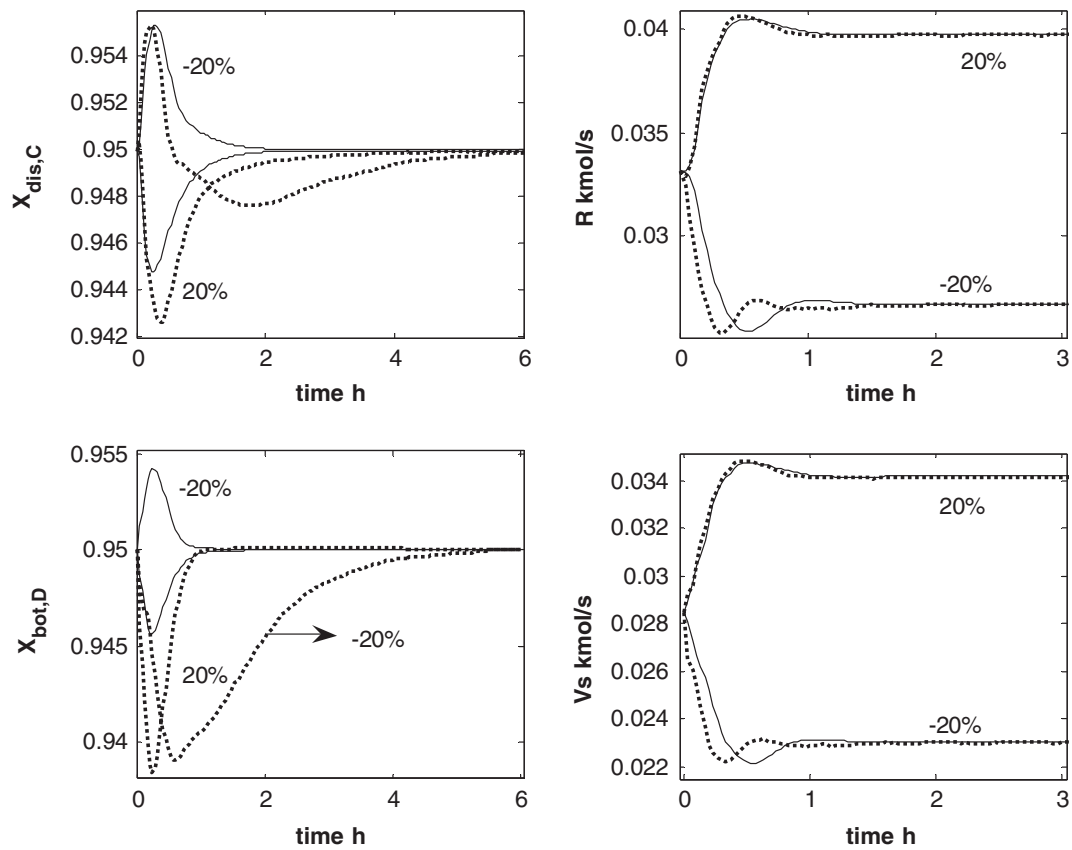

Fig. 4. Closed-loop performance when all of the composition controllers rely on the EKF: the base initial condition error, $\delta_m = 10\%$ and $\delta_p = 1\%$ are used for EKF design; +20% and −20% F_B disturbance; (—) CS-A, (- - - -) CS-E3.

For a setpoint tracking, the following changes are investigated:

(1) increase the product purity i.e., $x_{\text{bot},D} = x_{\text{dis},C} = 97\%$,
(2) decrease the product purity i.e., $x_{\text{bot},D} = x_{\text{dis},C} = 93\%$.

Fig. 4 compares the control performance of the system that relies on the state estimator (CS-E3) to that when a perfect analyzer is used (CS-A) when ±20% F_B changes are made. The results generally demonstrate that the controllers can successfully depend on the state estimates from the estimator for decision making. The estimator-based system is able to reject the disturbance and drive the system to the desired operating specifications.

The control performance of the estimator-based system is seen to be relatively poor a few moments after the start up when compared to the control performance using direct measurements from the online analyzer. The reason for this is because of a large estimation error at the start up as a result of the error in the initial conditions, measurement noise and plant–model uncertainties, which will require some times to be adjusted for. Because the gain matrix of the EKF is calculated and updated online, the response of the state estimator depends largely on system dynamics, disturbance input and the present initial condition error. This is why $x_{\text{bot},D}$ in CS-E3 control configuration moves in wrong direction at the early stage when a 20% decrease in F_B is introduced. To further justify this and appreciate the use of a state estimator in the control system of reactive distillation, the system is excited by a PRRS forcing function shown in Fig. 3. The result of the CS-E3 is compared to CS-A in Fig. 5. It can be seen clearly that after the state estimator overcomes the large estimation error occurring at the early stage of the process, the response of the CS-E3 system gives an excellent matching with that of CS-A, which indicates a good control performance. It is interesting to note that the same trend of disturbance in the first 6 h (i.e., +20% F_B in the first 3 h and −20% F_B in the next 3 h) of operation was repeated between the time of 10–16 h, but this time, the CS-E3 responds adequately and the system is effectively controlled. This is because at the later time, the estimator has already overcome the effect of the initial estimate error by updating the estimator gain.

The performance of the CS-E3 is investigated when a setpoint change in the products purity is desired. The products purity is changed by ±2% from the base purity of 95%. Fig. 6 compares the responses of the CS-E3 and to those of CS-A for these setpoint changes. These results demonstrate that setpoint changes of the products purity can be handled well by the CS-E3.

5.2. Effect of erroneous initial conditions

Because the actual initial conditions of the system are often not known in real situation, a state estimator must be designed

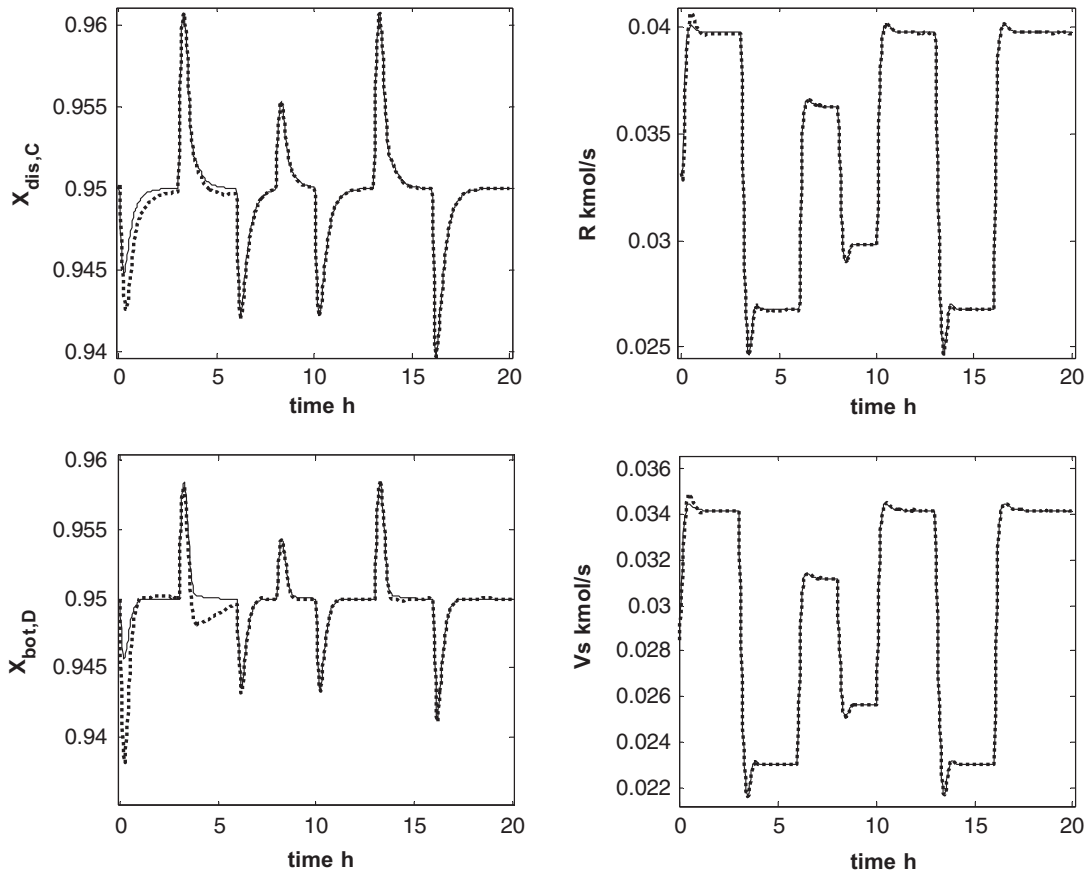

Fig. 5. Closed-loop performance when all of the composition controllers rely on the EKF: the base initial condition error, $\delta_m = 10\%$ and $\delta_p = 1\%$ are used for EKF design; F_B is a PRRS forcing function; (—) CS-A, (- - - -) CS-E3.

to be able to converge to the actual column state on time when it is initialized with guessed initial conditions. In practice, what matters most are a few moments after a change is introduced into the system as the control system will intervene to reject the disturbance. In order to investigate the impact of erroneous initial conditions on performance of the estimator and in turn, the control system as a whole, two set of erroneous initial conditions are tested as shown in Fig. 7a. The first set of initial conditions error is taken to be four times in magnitude the base initial conditions error ($4x_0$err), while the second set assumed an extreme case of equal composition of components in all of the stages (i.e., $\hat{X}(0) = 0.25/0.25/0.25/0.25$).

At first, the performance of the estimator in predicting the actual state is examined by simulating the open-loop dynamics of the system. This is to demonstrate that even though the estimator might be able to converge to the actual state at the long run using the worst set of initial conditions, the estimator accuracy at the early stage of the start up is important to the control system that relies on the state estimator. In the open-loop dynamics, all of the composition controllers are on manual, while the level controllers are automatic. In this test, the forcing function is a 20% increase in feed flowrate of reactant B, while the base initial conditions error, measurement and plant noise are used in the EKF design. Fig. 7b shows the performance of the state estimator to different set of initial conditions. Though, this result illustrates the capability of the state estimator to start from guessed initial conditions and converge to the correct states, however, it shows that the closer the initial estimates (provided to the estimator) to the actual initial conditions, the better the performance.

The same set of initial conditions is then used to simulate the CS-E3 system. Fig. 8 shows the control performance when F_B is changed by $\pm 20\%$. The CS-E3 behaves predictably well in disturbance rejection when the first set of erroneous initial conditions is used. However, the CS-E3 behaves poorly and unable to control the system when equal composition of components is used as the initial estimates. Although the open-loop system responses shown in Fig. 7b suggests that the filter will be able to converge to the correct states at a longer period of time, but in the closed-loop mode, the state estimates from the filter at the early stage determines the performance of the controllers. Because the controllers use extremely poor estimated states a few moments after the startup, the controlled variables are driven too far from the required setpoint, and thus lead to control system failure.

Therefore, to achieve an effective control system, it is important to reduce the difference between the actual and the estimated data in the short time possible following a disturbance so

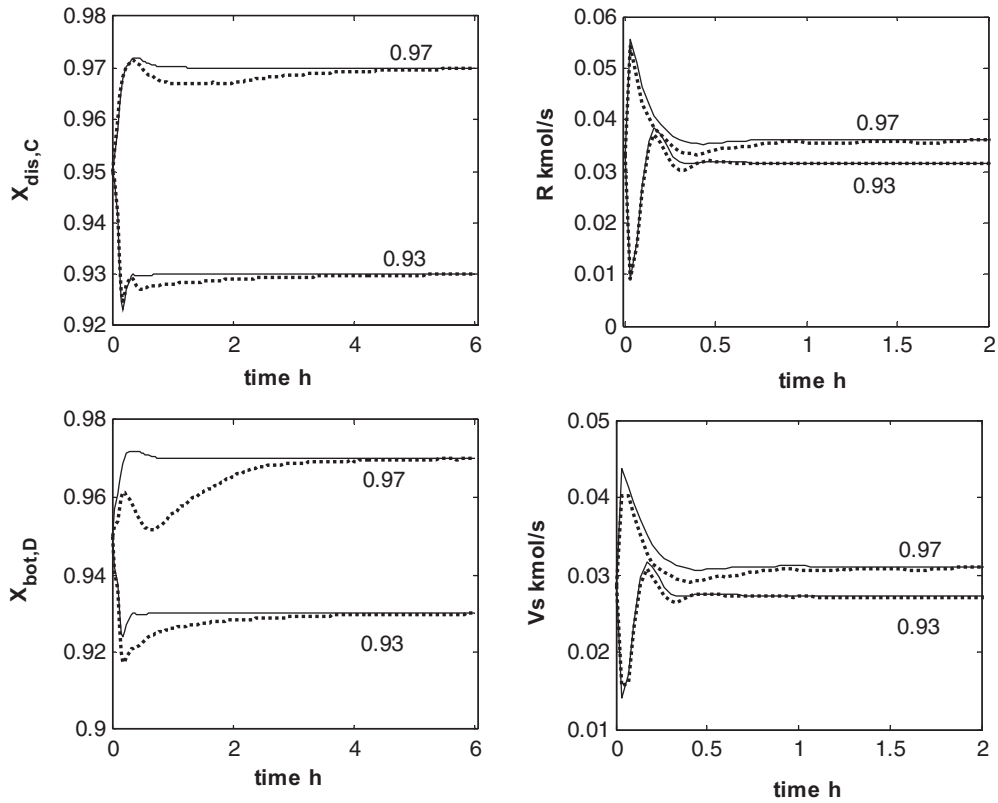

Fig. 6. Closed-loop performance to setpoint changes when all of the controllers rely on the EKF: $X_{\text{bot},B}$ and $X_{\text{dis},C}$ from 95% to 93% and from 95% to 97%; the base initial conditions error, $\delta_m = 10\%$ and $\delta_p = 1\%$ are used for EKF design; (—) CS-A, (- - - -) CS-E3.

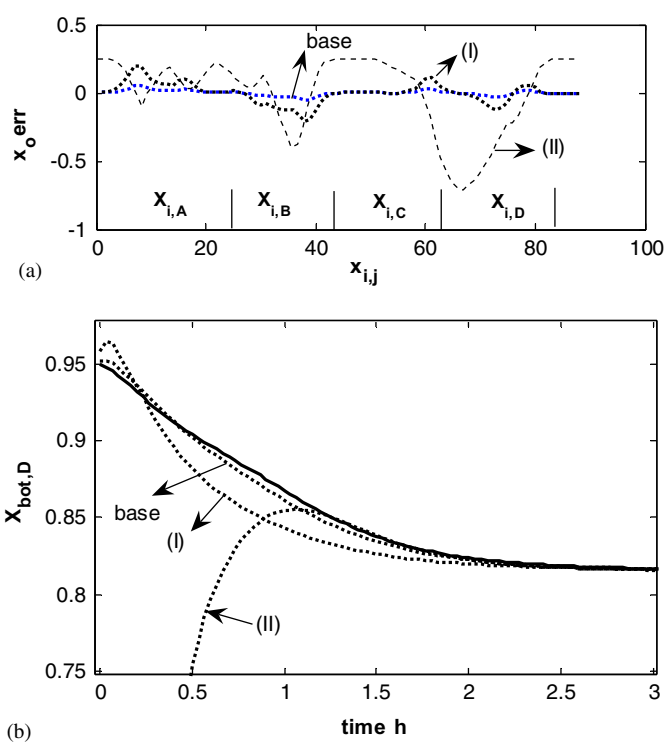

Fig. 7. Open-loop performance under the erroneous initial conditions with a 20% F_B disturbance: (a) base ($\hat{X}(0) = X_0 + x_0\text{err}$), (I) $\hat{X}(0) = X_0 + 4x_0\text{err}$, (II) $\hat{X}(0) = 0.25/0.25/0.25/0.25$; (b) open-loop system response; (—) actual state, (- - - -) estimated state; $\delta_m = 10\%$ and $\delta_p = 1\%$ are used for EKF design.

that the estimated data that the controllers use are close enough to the actual plant data. One of the ways to do this is to use approximate initial conditions close enough to the true initial conditions of the actual system for the state estimators.

5.3. Effect of measurement errors

In this section, we are interested in assessing the effect of cyclical errors in the temperature measurements. Unlike measurement noise, which is a stochastic and nondeterministic error of the sensors that cannot be predicted, cyclical errors are the result of sensors imperfections and/or abnormal performance due to inaccurate settings. These types of errors are deterministic and repeatable. Fig. 9 compares the control performance of CS-E3 to that of CS-A when 1 °C measurement error is introduced in each of the sensors located in the reboiler, tray nf1 and the top plate. The system is excited through implementing the PRRS forcing function on F_B (see Fig. 3). The CS-E3 performs reasonably well in resisting the effect of the disturbance with an acceptable error in the desired compositions.

Generally, the end effect of the sensors errors depends on the error type. This can be best explained when considering how well the estimator is able to predict the actual column temperature based on the noise-contaminated temperature data supplied by the sensors. This is illustrated in Fig. 10, by comparing tray nf1 temperature measured by the sensor (T_{meas}) and as predicted by the state estimator (T_{est}) to the actual

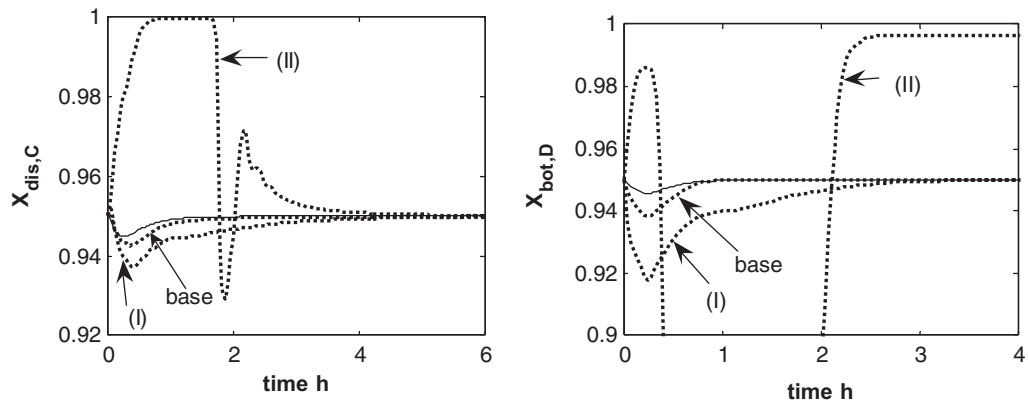

Fig. 8. Closed-loop performance under the erroneous initial conditions with a +20% F_B step change (I) $\hat{X}(0) = X_0 + 4x_0\text{err}$, (II) $\hat{X}(0) = 0.25/0.25/0.25/0.25$; $\delta_m = 10\%$ and $\delta_p = 1\%$ are used for EKF design; (—) CS-A, (- - - -) CS-E3.

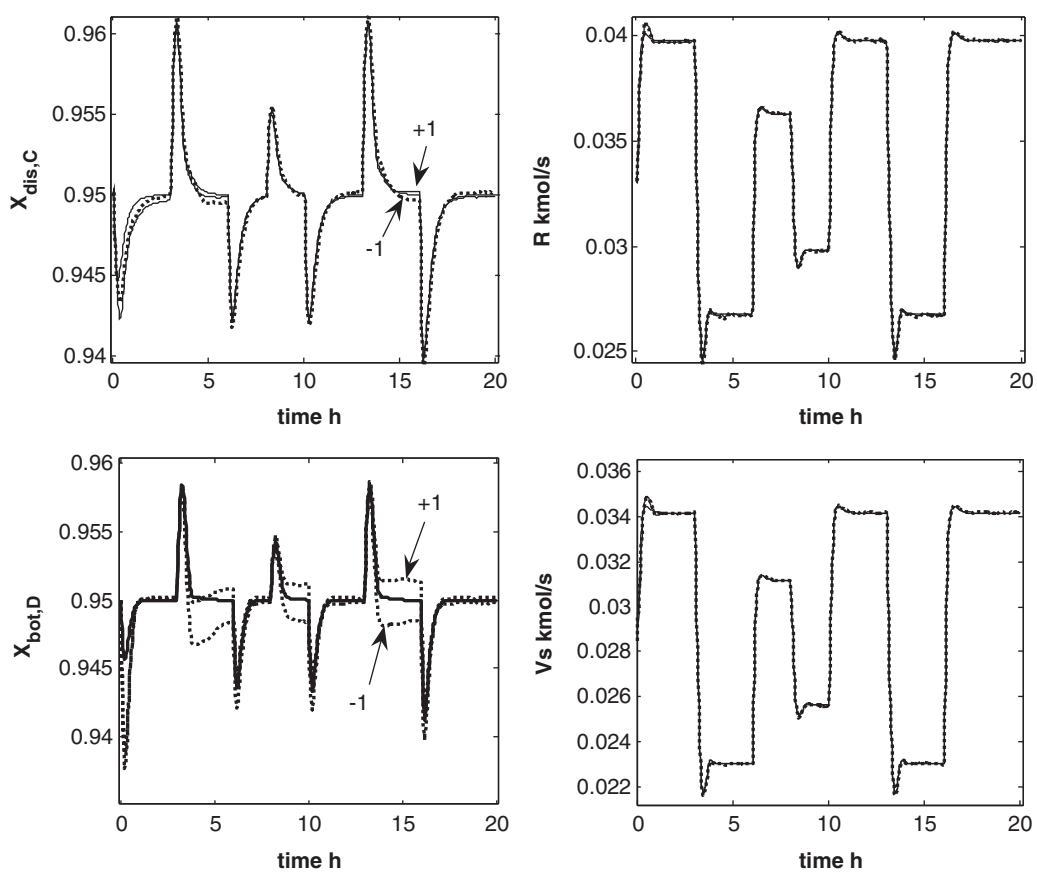

Fig. 9. Closed-loop performance when all of the controllers rely on the EKF in presence of the temperature measurement error of ±1 °C with PRRS disturbance on F_B: the base initial condition error, $\delta_m = 10\%$ and $\delta_p = 1\%$ are used for the EKF design; (—) CS-A, (- - - -) CS-E3.

temperature profile (T_{actual}). It can be seen that the high-frequency noise was effectively attenuated by the built-in filter in the state estimator, but the effect of the 1 °C bias (deterministic error) in the measurement data was only reduced and not eliminated. Because the control system is designed to follow the feedback signal from the state estimator (including its estimated errors) as much as possible, deterministic errors will carry through, at least in part, to the control system and corrupt the response output. Therefore, efforts must be given to using accurate sensors with minimal cyclical errors when implementing the estimator-based control system.

5.4. Plant–model mismatch

Though reactive distillation systems are generally known to have many advantages over the conventional multi-unit

reaction/separation/recycle systems, they often possess complex dynamics and limited flexibility because of the interactive effect of reaction on separation. For a state estimator that relies heavily on such system dynamics, the effect of plant–model mismatch is essential to be investigated. It has also been reported in the literature that the plant–model mismatch has considerable effects on the performance of state estimator in a closed-loop nonlinear distillation process (Ruokang and Olson, 1991). The effect of plant–model mismatch on the estimator-based control performance of our system is studied by considering the state estimator designed from a two different process models:

(1) A linearized process model.
(2) A nonlinear process model with significant errors in some process parameters.

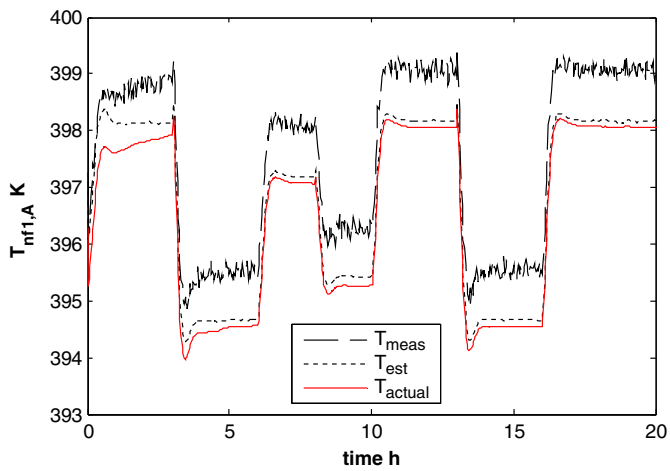

Fig. 10. Temperature profile on tray nf1 of the CS-E3 with a measurement error of 1 °C in the thermocouples located on the reboiler, the tray nf1 and the top plate; the base initial condition error, $\delta_m = 10\%$ and $\delta_p = 1\%$ are used for the EKF design.

5.4.1. Linear process model

The nonlinear model of Eqs. (12) and (13) can be linearized around the desired operating conditions by the Taylor series expansion method to obtain an approximate linear process model of the form:

$$\dot{X}(t) = AX(t) + BU(t) + Ed(t) + w(t), \tag{24}$$

$$Z = CX(t) + v(t). \tag{25}$$

The w and v are vectors of the plant and measurement noise, while the transition matrices A, B, C and E are evaluated at the desired steady-state operating conditions. Therefore,

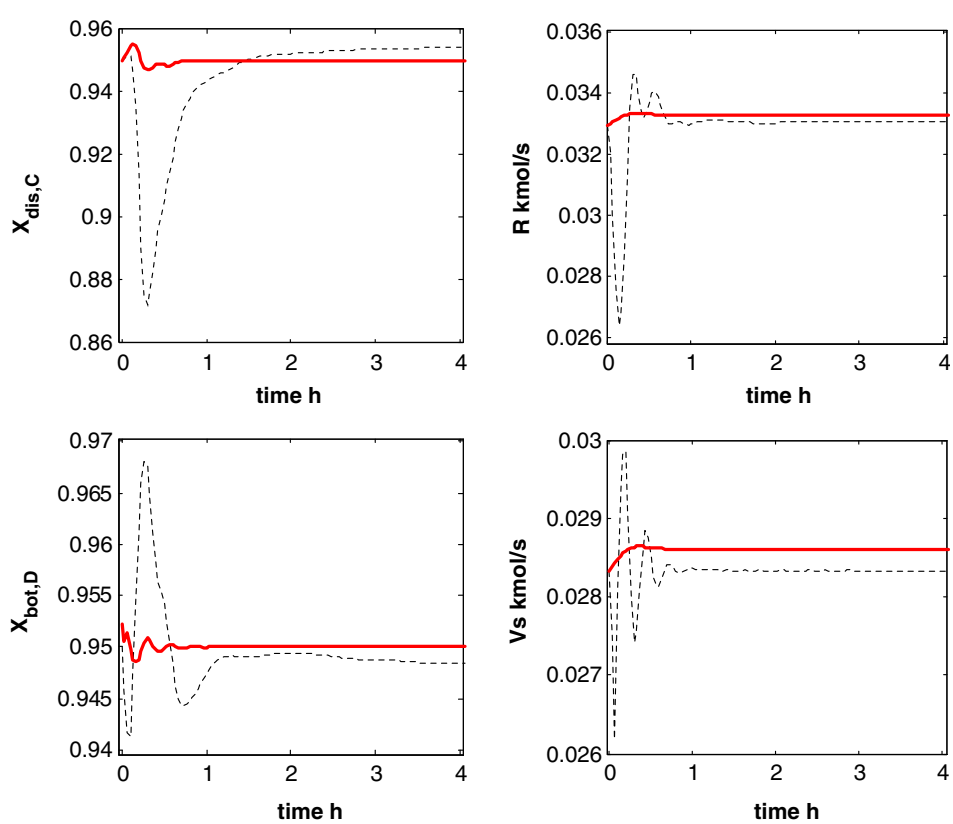

Fig. 11. Closed-loop performance of a nonlinear system that relies on linear estimator when all of the controllers rely on the EKF with a 1% F_B disturbance: the base initial condition error, $\delta_m = 10\%$ and $\delta_p = 1\%$ are used for the EKF design; (—) CS-A, (- - - -) CS-E3.

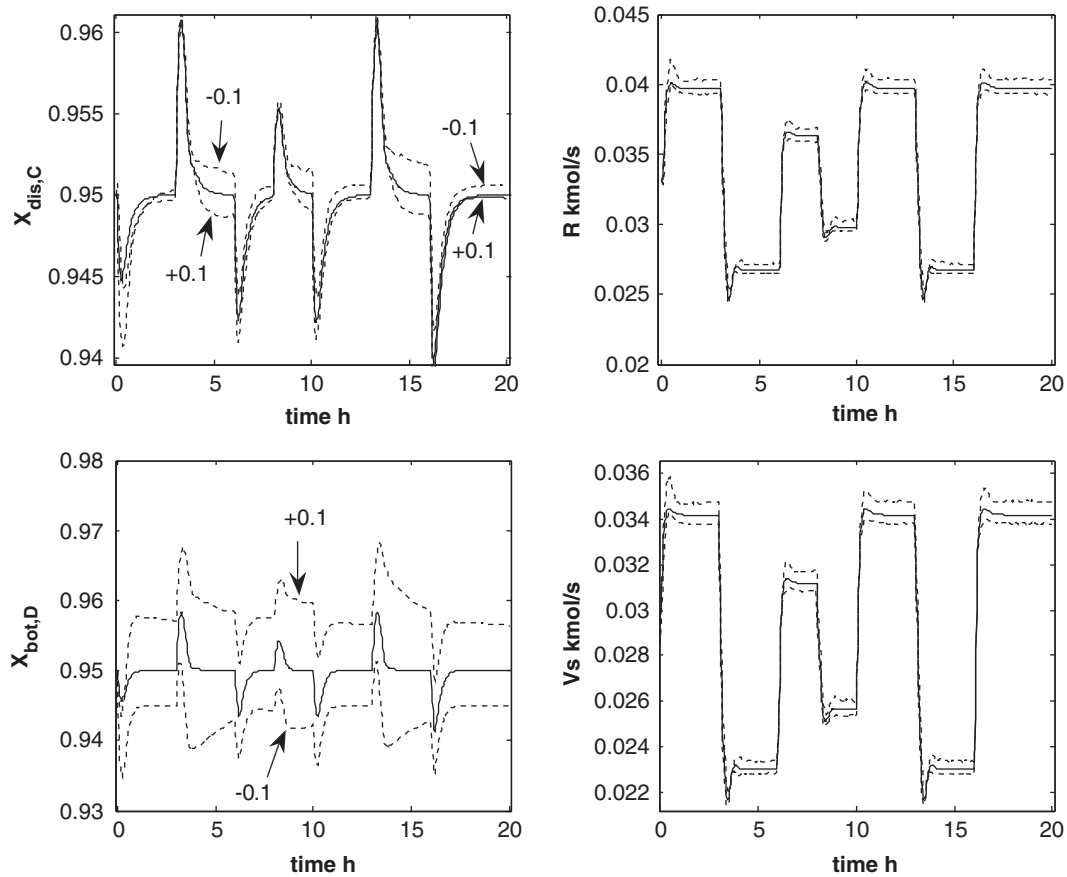

Fig. 12. Closed-loop performance under the error in the relative volatility with a PRRS forcing function on F_B: the base initial condition error, $\delta_m = 10\%$ and $\delta_p = 1\%$ are used for EKF design; (—) CS-A, (- - - -) CS-E3.

the components of a linear estimator can be summarized as follows:

$$\hat{X}(0) = X_0 + x_0\text{err}, \tag{26}$$

$$Y = C\hat{X}(t), \tag{27}$$

$$\dot{\hat{X}}(t) = A\hat{X}(t) + BU(t) + Ed(t) + K[Z(X(t)) - Y(\hat{X}(t))]. \tag{28}$$

In a practical situation, the linearized process model will not be a perfect representation of the actual plant and the applicability of the linear estimator into a realistic system might be restricted (i.e., limited operating conditions and small magnitude of disturbance input). In order to investigate the feasibility of applying the linear estimator into a practical system, the developed linear estimator is directly implemented in a reactive distillation represented by the nonlinear system.

The nonlinear system presented in Section 2 is considered as the real plant model and the state composition as predicted by the linear estimator are fed back into the controllers. Fig. 11 shows the closed-loop nonlinear system performance when all of the three controllers rely on the linear estimator. The disturbance input is just a 1% increase in feed flowrate of reactant B. The controllers that relied on the estimates from the linear estimator perform inadequately in driving the system to the required specifications. The result demonstrated that a linear estimator would be inappropriate to a real system when the plant–model mismatch is significant.

5.4.2. Nonlinear process model with significant error in process parameters

Uncertainties in relative volatility have significant effects on the design and performance of reactive distillation (Kaymak and Luyben, 2004a,b). Therefore, inaccurate modeling of the reaction kinetics and vapor–liquid equilibrium (VLE) relation can consequently affect the performance of the state estimators (Baratti et al., 1995, 1998). To illustrate this, we have considered the effect of errors in the components relative volatilities, which in practice, are usually known with some uncertainty. The relative volatilities of the components in the real plant model are given in Table 1. Two set of erroneous relative volatilities are tested as follows:

(I) $\hat{\alpha} = 3.9/1.9/7.9/1$, where -0.1 is added in the component relative volatilities.
(II) $\hat{\alpha} = 4.1/2.1/8.1/1$, where $+0.1$ is added in the component relative volatilities.

Using these set of relative volatilities in the estimator model means that the system dynamics has been altered by

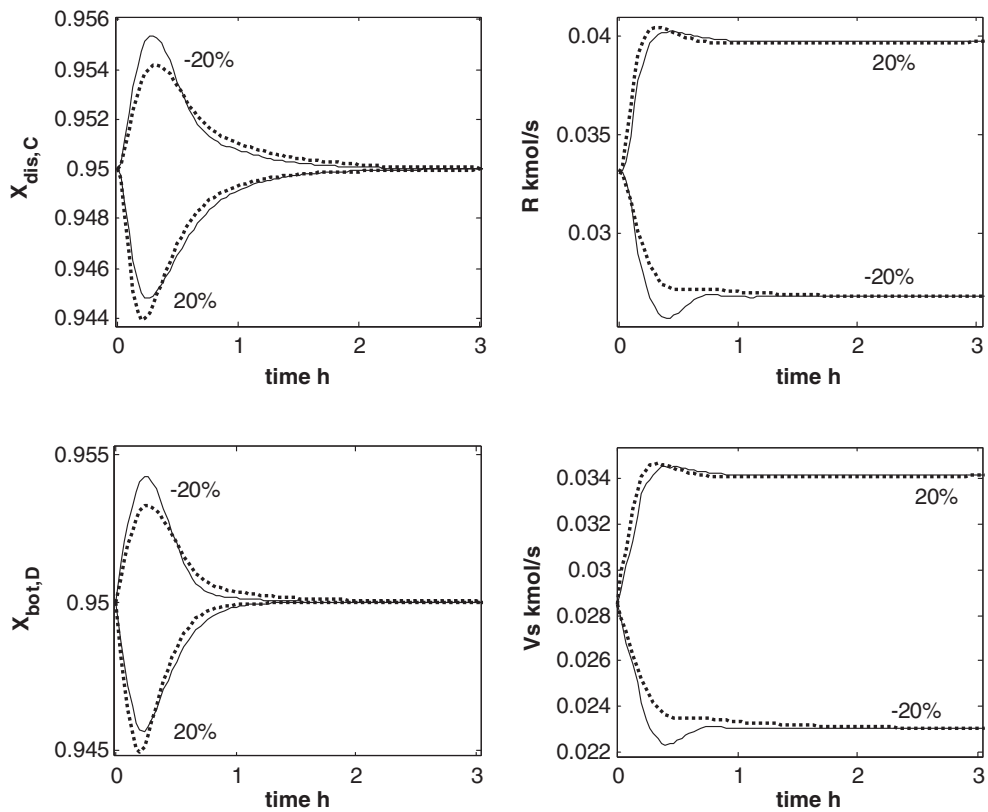

Fig. 13. Closed-loop performance when only internal composition controller relies on the EKF (CS-E1): the base initial condition error, $\delta_m = 10\%$ and $\delta_p = 1\%$ are used for EKF design; +20% and −20% F_B disturbance; (—) CS-A; (- - - -) CS-E1.

inaccurate vapor–liquid relationship parameters. The resulting control performance of CS-E3 under the effect of erroneous relative volatilities is shown in Fig. 12. It can be seen clearly that an inaccurate VLE representation has a major effect on the control performance of the CS-E3 system. Therefore, an adequate representation of the VLE relations is very important and a necessity to the successful application of the estimator in the control system of reactive distillation.

5.5. Control performance under special conditions

Even if an online analyzer is available and poses no problem in measuring the product composition at the two ends of the column, the internal composition will still be difficult to obtain using an online analyzer and thus will make the use of an online estimator inevitable. Therefore, an alternative control configuration is studied where a state estimator is used to estimate only the inaccessible internal composition, while the distillate and bottoms composition controllers use online perfect analyzers. This control system is termed "CS-E1". Fig. 13 shows the responses of a CS-E1 and a CS-A when ±20% changes are made. Comparing the results shown in Fig. 13 to those in Fig. 4, it can be easily noticed that the system generally demonstrates a better performance when only the internal composition controller relies on the estimator. The response of $x_{\mathrm{bot},D}$ moves in the expected direction because the bottom composition controller does not depend on the estimator and the overall effect of the large estimated error at the early stage of operation is significantly reduced.

Motivated by the performance of the CS-E1 when only the internal composition controller relies on the prediction by the estimator as discussed earlier, one would be curious at this point to examine the control performance of CS-E1 and CS-E3 but when the estimator is designed under severe bad conditions, which are:

1. Measurement and plant noise: $\delta_m = 10\%$, $\delta_p = 1\%$.
2. Measurement bias of 2 °C for thermocouples located in the reboiler, tray nf1 and the top plate.
3. Initial conditions error: $4x_0$err.
4. Error in relative volatility: $\hat{\alpha} = 4.2/2.2/8.2/1$.
5. A PRRS forcing function on F_B.

Fig. 14 compares the responses of CS-E1 and CS-E3 under these conditions to those of CS-A. As can be seen, the CS-E1 i.e., when only the internal composition controller relies on the state predicted by the EKF, provides a good control of the system. On the other hand, the CS-E3 performance is poor as the products purity is not adequately maintained to the required specification. This result shows that a state estimator designed from a highly erroneous process model, noisy measurements and approximate initial conditions could be used together with an online analyzer (for easily measured states) to achieve an effective control system of a reactive distillation.

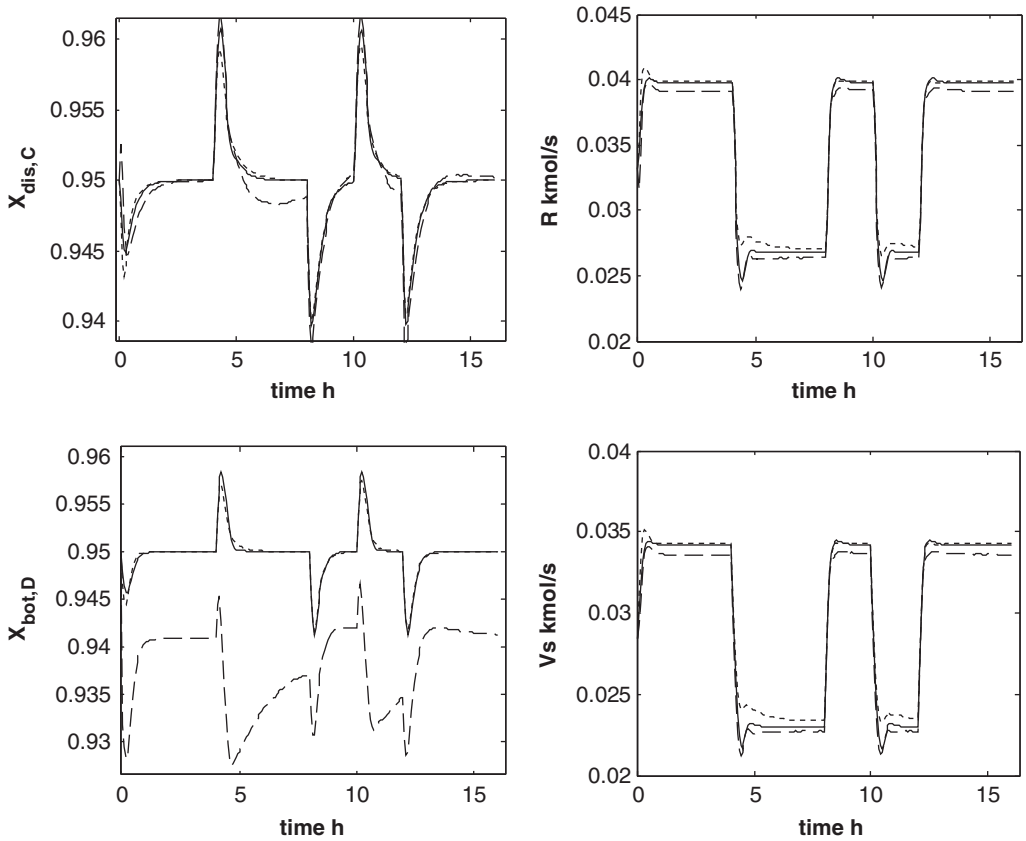

Fig. 14. Closed-loop performance under the special conditions of a PRRS forcing function on F_B, temperature measurement error of 2 °C, $\hat{X}(0) = X_0 + 4x_0\text{err}$ and $\hat{\alpha} = 4.2/2.2/8.2/1$ are used in the EKF design; $\delta_m = 10\%$, $\delta_p = 1\%$; (—) CS-A, (—-) CS-E1, (- - -) CS-E3.

6. Conclusion

In this work, we have shown that an estimator-based control system can be implemented on reactive distillation process. The control performance of the system that relies on the state estimator is compared to that of the system which takes direct measurement from the process assuming the availability of perfect online analyzer. The reliability of an extended Kalman filter is examined through the performance of the estimator-based system in the presence of the measurement errors, model uncertainties and erroneous initial conditions.

Generally, the estimator-based control system will give a good performance when an accurate process model of a system can be obtained and the effect of the measurement errors can be minimized. However, if the process model used to design state estimator contains a significant plant–model mismatch, it is recommended to minimize the use of the state estimator to predict only the inaccessible states.

Notation

A	reactant component
A	matrix of state variables of the linearized process
B	matrix of inputs of the linearized process
B	reactant component
C	matrix of outputs of the linearized process
C	product component
d	disturbance variables vector
EKF	extended Kalman filter
F_A	fresh feed flowrate of reactant A, kmol/s
F_B	fresh feed flowrate of reactant B, kmol/s
F_i	fresh feed flowrate on tray i, kmol/s
K	gain matrix
K_B	specific reaction rate of the reverse reaction, kmol/s/kmol
K_F	specific reaction rate of the forward reaction, kmol/s/kmol
L	liquid flowrate, kmol/s
M_i	liquid holdup in all stages, kmol
nf1	first tray of reactive section (entrance of feed F_A)
nf2	last tray of reactive section (entrance of feed F_B)
N	total number of stages including reboiler and reflux drum
N_R	rectifying section
N_{RX}	reactive section
N_S	stripping section
P	column pressure
R	reflux flowrate, kmol/s
R_i	rate of production on tray i, kmol/s

T_{actual}	actual temperature from the plant model
T_{est}	estimated temperature
T_i	temperature in stage i, K
T_{meas}	measured temperature by the sensor
U	input variables vector
v	measurement noise
V_i	vapor flowrate on tray i, kmol/s
V_S	vapor flowrate from the reboiler, kmol/s
w	plant noise
$x_{i,j}$	liquid mole fraction of component j on tray i
$x_0$err	initial condition error vector
X	vector of the state variables
$X_{\text{bot},D}$	composition of D in the bottoms
$X_{\text{dis},C}$	composition of C in the distillate
$X_{\text{nf1},A}$	composition of A in tray nf1
X_0	initial conditions of the plant model
$\hat{X}$	state estimate vector
Y	output vector
$\hat{Y}$	observation vector
Z	measured output vector
$Z_{i,j}$	composition of fresh feed j on tray i

Greek letters

α_j	relative volatility of component j with respect to heavy component
$\hat{\alpha}$	approximate relative volatility
δ_m	standard deviation of the measurement noise
δ_p	standard deviation of the plant noise
ΔH_v	heat of vaporization, cal/mol
θ	lumped model parameters
λ	heat of reaction, cal/mol

Acknowledgements

The authors acknowledge King Fahd University of Petroleum & Minerals, Dhahran, Saudi Arabia, for funding this research.

References

Al-Arfaj, M.A., Luyben, W.L., 2000. Comparison of alternative control structures for an ideal two-product reactive distillation column. Industrial and Engineering Chemistry Research 39, 3298–3307.

Al-Arfaj, M.A., Luyben, W.L., 2002a. Control study of ETBE reactive distillation. Industrial and Engineering Chemistry Research 41, 3784–3796.

Al-Arfaj, M.A., Luyben, W.L., 2002b. Comparative control study of ideal and methyl acetate reactive distillation. Chemical Engineering Science 24, 5039–5050.

Al-Arfaj, M.A., Luyben, W.L., 2002c. Control of ethylene glycol reactive distillation column. A.I.Ch.E. Journal 48, 905–908.

Al-Arfaj, M.A., Luyben, W.L., 2004. Plantwide control for TAME production using reactive distillation. A.I.Ch.E. Journal 50 (7), 1462–1473.

Baratti, R., Alberto, B., Alessandro, D.R., Massimo, M., 1995. Development of a composition estimator for binary distillation columns. Application to a pilot plant. Chemical Engineering Science 50, 1541–1550.

Baratti, R., Alberto, B., Alessandro, D.R., Massimo, M., 1998. A composition estimator for multicomponent distillation columns development and experimental test on ternary mixtures. Chemical Engineering Science 53, 3601–3612.

Bisowarno, B.H., Tian, Y.-C., Tade, M.O., 2003. Model gain scheduling control of an ethyl *tert*-butyl ether reactive distillation column. Industrial and Engineering Chemistry Research 42, 3584–3591.

Gruner, S., Mohl, K.-D., Kienle, A., Gilles, E.D., Fernholz, G., Friedrich, M., 2003. Nonlinear control of a reactive distillation column. Control Engineering Practice 11, 915–925.

Kaymak, D.B., Luyben, W.L., 2004a. Effect of relative volatility on the quantitative comparison of reactive distillation and conventional multi-unit systems. Industrial and Engineering Chemistry Research 43, 3151–3162.

Kaymak, D.B., Luyben, W.L., 2004b. Effect of the chemical equilibrium constant on the design of reactive distillation columns. Industrial and Engineering Chemistry Research 43, 3666–3671.

Luyben, W.L., 2000. Economic and dynamic impact of the use of excess reaction in reactive distillation systems. Industrial and Engineering Chemistry Research 39, 2935–2946.

Monroy-Loperena, R., Alvarez-Ramirez, J., 2000. Output-feedback of reactive batch distillation columns. Industrial Engineering Chemistry Research 39, 378–386.

Oisiovici, R.M., Cruz, S.L., 2000. State estimation of batch distillation columns using an extended Kalman filter. Chemical Engineering Science 55, 4667–4680.

Ruokang, L., Olson, J.H., 1991. Fault detection and diagnosis in a closed-loop nonlinear distillation process: application of extended Kalman filters. Industrial and Engineering Chemistry Research 30, 898–908.

Sorenson, H.W., (Ed.), 1985. Kalman Filtering: Theory and Application. IEEE Press, New York.

Vora, N., Daoutidis, P., 2001. Dynamics and control of an ethyl acetate reactive distillation column. Industrial and Engineering Chemistry Research 40, 833–849.

Wang, S., Wong, D.S., Lee, E., 2003. Control of a reactive distillation column in the kinetic regime for the synthesis of *n*-butyl acetate. Industrial and Engineering Chemistry Research 42, 5182–5194.